Fog Events at Maceio Airport on the Northern Coast of Brazil During 2002–2005 and 2007

Natalia Fedorova,[1] Vladimir Levit,[1] José Leonaldo de Souza,[1] Aliton Oliveira Silva,[1] Joao M. Sousa Afonso,[1] and Iedo Teodoro[1]

Abstract—There were eight fog events in five years at Maceio international airport on the northern coast of Brazil, and all were analyzed. Fog duration was short and its intensity was weak or moderate. The principal objectives of the study were: (1) analysis of the physical processes of fog formation (synoptic and thermodynamic conditions and processes), (2) PAFOG model testing, and (3) estimation of the effect of vegetation on fog forecast. Cyclonic curvature and divergence of the air current over the ocean at low levels and anticyclonic curvature at high levels were associated with the fog. Weak lifting at low levels was identified by the NCEP/DOE II, ECMWF, and WRF models for all eight events. Sinking at high levels was dominant in the ECMWF and WRF models. Absence of thermal inversion and conditional instability at low levels was identified by the NCEP/DOE II and ECMWF models. According to the WRF model a typical temperature profile during fog comprises three layers: (1) a very thin layer (up to 166 m, 985 hPa) of temperature inversion with very high humidity; (2) a conditional layer of instability from 985–860 hPa; and (3) a dry and stable layer above 860 hPa. Moderate fog with visibility between 200 and 300 m was associated with ocean cooling whereas weak fog was associated with ocean warming. A warm oscillation on the sea surface near the Brazilian northeast was observed for all fog events. It was found there was colder air over the warmer water near the coast. Weak confluence in troughs at low levels contributes to weak lifting at low levels. This current creates conditions resulting in humidity increase. A warmer sea surface contributes to more evaporation and, as a consequence, increases the amount of water vapor in the surrounding air at low levels near the coast. The PAFOG model was used to forecast the fog for three events (i.e., for all cases possible), and was satisfactory for two cases. Satisfactory results for fog duration and intensity were obtained with 9 h of antecedence. No significant effect of fast-growing sugarcane on the low visibility forecast was detected.

Key words: Fog formation, thermodynamic analysis, PAFOG model, tropical region, sea surface temperature.

1. Introduction

Fog and stratus clouds are very rare on the northern coast of Brazil (Fedorova *et al.* 2008; Gomes *et al.* 2011), but one incident of intense fog caused a fatal airplane accident near the Maceio Airport in 2007 (Fedorova *et al.* 2013). This fog and all other occurrences of fog during 5 years were not predicted by the Terminal Aerodrome Forecast messages because of the absence of a fog forecast method for this region.

Fog formation was studied during the last century. One of the first important studies of the physical processes of fog formation was performed by Willett (1928), and the principal fog formation types, for example radiation, advection, and frontal, were described. The Petersen classification (1956) was based on the principal fog-formation processes, for example evaporation, cooling, and mixing. Byers *et al.* (1959) added the process of evaporation from humid surfaces as an important mechanism of fog development. The absence of thermal inversion near the surface during fog and its existence between 100 and 600 m were also discussed, for the first time.

The effect of dew, turbulence, vegetation, and cloud advection has been described by Cotton and Anthes (1989), according to whom cloud advection changes the radiation balance and surface temperature. Surface deposition of dew is responsible for humidity transport and dew inversion formation at heights of 40 and 200 m (Cotton and Anthes 1989). During sunrise, temperature increase and the process of dew evaporation occur more quickly, until dew evaporation is complete and no dew remains.

Turbulence helps to reduce surface humidity and the possibility of dew formation and, therefore, vertical turbulent mixing prevents fog formation

[1] Institute of Atmospheric Science, Federal University of Alagoas-UFAL, Campus A. C. Simões, Av. Lourival Melo Mota, 57072-900 Maceió, Alagoas, Brazil. E-mail: natalia@dimin.net

(Cotton and Anthes 1989). Several effects of turbulence on fog formation can be described by the so-called critical turbulent exchange coefficient (Kc), which defines the upper limit of the turbulence intensity (Zhou and Ferrier 2008). Two factors can cause the turbulence intensity to exceed Kc:

1. a reduction in the rate of cooling because of sunrise, local clouds, and warm advection; and
2. increasing local wind speeds, which increase surface mechanical turbulence (Kc increases).

Kc can be used as a threshold for prediction of whether a fog persists or dissipates. Fog development has been shown to be very sensitive to turbulence generation (Welch and Ravichandran 1986). The surface layer varies from lapse conditions to strong surface inversion, which is observed after sundown when turbulence generation is suppressed. Increased turbulent mixing rapidly lifts the surface inversion. Fog top height is directly correlated with the height of this inversion.

Microphysics processes also affect visibility in fog. For example, advection fog droplet size data have been used to determine extinction coefficients and mean terminal velocities as functions of liquid water content (LWC) and droplet concentrations (Kunkel 1984). The results revealed higher liquid water content and extinction coefficients and lower mean droplet sizes at 30 m than at 5 m. The relationship between the extinction coefficient and LWC was more linear than that found by other investigators. In general this results in lower extinction coefficients for liquid fogs and higher extinction coefficients for dense fogs for a given LWC than extinction coefficients determined by use of other relationships.

Vegetation type affects surface cooling, which, in turn, promotes fog formation (Cotton and Anthes 1989). Vegetation height, shielding, and leaf type are associated with the stage of development of vegetation and therefore vary during the year. The type of the vegetation determines the albedo, minimum stomata, and maximum water storage of the foliage.

Climatological data for the northern coast of Brazil reveal substantial variation of fog frequency. Radio-sound data from the nearest meteorological stations to Maceio city, at Recife and Salvador, are indicative of fog on 13 and 37 days/year, respectively, on average (Ratisbona 1976). In the first study of fog formation in Maceio, however, Silveira (2003) observed only two incidences of fog (moderate and weak) during 1996 (both in winter). Different fog duration and frequencies of formation on the northern and southern coasts of Brazil have been reported by Fedorova et al. (2008). Fog duration was 1–2 h on average on the northern coast and 12 h on the southern coast. Fog on the southern coast is typical radiation fog, i.e. fog formed at high levels during nights without clouds because of radiation temperature decreases. Fog on the northern coast is atypical. The processes of formation of this type of fog will be discussed in this paper.

Maceio is located on the coast and it is, therefore, important to study the effect of the ocean. After an investigation of sea fog formation over the Yellow and Bohai Seas in China the problem was described from the different perspectives of observational analysis and high-resolution modeling of sea fog (Fu et al. 2012). This book defines sea fog as a type of advection fog which occurs when air lying over a warm water surface is transported over a colder water surface, resulting in a cooling of the lower layer of air below its dew point. Oceanic and synoptic features create the conditions for fog formation. It was reported that weak winds, stable conditions and a continuous supply of moist air are necessary for formation of sea fog. The authors of the book used the physical basis of the high-resolution Regional Atmospheric Modeling System model for fog forecasting and used it to forecast dense sea fog events. Maritime and coastal fog is connected frequently with the advection process. In the classic process of advection sea fog formation, warm moist air is transported from the land surface as a stable layer and this warm air cools over the cold sea. Dissipation of sea fog can be the result of the following processes:

1. fog movement over warmer water;
2. movement of cloud cover over the fog; and
3. fog advection on the continent over the drier and warmer surface.

Warm waters often inhibit fog formation and contribute to its dissipation when fog is advected over

warmer waters. Fog is not formed over a very warm water surface for two main reasons:

1. thermal convection development, weakening thermal inversion; and
2. because vapor pressures increase as temperatures rise, higher concentrations of water vapor are required to reach saturation and condensation.

Association of fog formation with synoptic scale processes, for example high and frontal zones, has been described in a variety of synoptic research papers; examples include PETTERSSEN (1956) and GUSEVA and RAZIMOR (1986). This relationship has been studied in detail for extra-tropical regions. Others synoptic scale systems are observed in the tropical region. The relationship between baric troughs and adverse meteorological phenomena (fog and thunderstorms) in Alagoas State has been studied by RODRIGUES et al. (2010). It was noted that 87 % of the troughs were associated with wave disturbances in trade winds (WDTW) on the northwestern periphery of the subtropical South Atlantic High. Fog formation is usually associated with the WDTW in Maceio (FEDOROVA et al. 2008). Moreover, stratus clouds were observed on the cold front periphery, at the easterly wave, and under the upper tropospheric cyclonic vortex.

Vertical profiles of the temperature and dew point of fog/stratus events have been studied on the northern and southern coast of Brazil (FEDOROVA et al. 2008). An intense inversion or stable layer with high humidity up to 950–670 hPa was associated with fog development on the southern coast. Radiation fog formation in a coastal region of southern Brazil has been studied by sounding (PIVA and FEDOROVA 1999) and two types of the vertical profile were determined. They are distinguished by:

1. temperature inversion;
2. a moist layer at low levels and a dry layer in the rest of the atmosphere; and
3. wind velocity at the earth's surface.

No stable layers or a very narrow humid layer were observed in all cases on the northern coast (FEDOROVA et al. 2008, 2013). The absence of an inversion layer and weak lifting at low levels were typical for this tropical region. In this region, the stratus clouds and fog were observed together with altostratus and cumulus clouds with weak convective available potential energy (CAPE) development above 950 hPa (CAPE was 370 J/kg, on average). The principal atmospheric conditions of an intense fog event in Maceio on the northern coast of Brazil were studied by FEDOROVA et al. (2013) and were:

– calm conditions, which provoke a reduction of horizontal visibility from 15 to 1.5 km within 1 h;
– radiation night cooling before sunrise;
– thermal inversion near the surface (height 30 m); atmospheric instability above 925 hPa; and
– weak lifting at low levels and sinking at middle–high levels.

Significant efforts have been made to forecast fog/low visibility. For example, a short-term (6 h only) method for forecasting visibility and low clouds at Paris's Charles de Gaulle International Airport was developed by BERGOT et al. (2005). Specific local observations and a detailed numerical 1D model were integrated into this method. The assimilation scheme follows three steps:

1. estimation of atmospheric profiles on the basis of a one-dimension variation framework;
2. correction of atmospheric profiles when fog and/or low clouds are observed; and
3. estimation of soil profiles to maintain consistency between soil profiles and the atmospheric state.

Inspection of the events indicates that improvement of very short-term forecasts is a consequence of the ability of the system used for forecasting to characterize the boundary layer processes more accurately, especially at night. This study also demonstrated that the use of a 1D model in a fog and low clouds forecast could be beneficial only if it is associated with local measurements and assimilation scheme. This study also showed that an integration of model and local observations is of crucial importance for development of forecasting methods. The main forecast problem is related to the low-level clouds, which are very sensitive to mesoscale flow (particularly subsidence). This investigation also showed that a 1D model can be an alternative tool for forecasting such local conditions as visibility, cloud ceiling, and boundary layer variables.

A new warm-fog visibility parameterization scheme for numerical weather-forecasting models was suggested by GULTEPE et al. (2006). Experimental information about boundary layer low-level clouds was used in their work to develop a parameterization scheme between visibility and a combined parameter as a function of both droplet number concentration and LWC. The current numerical models usually use relationships between the extinction coefficient and LWC. A newly developed parameterization scheme for visibility was applied to the NOAA Nonhydrostatic Mesoscale Model. A detailed microphysical scheme, adapted from the 1D PAFOG model and used in the 3D NMM fog model, significantly improved visibility calculations with the new parameterization (GULTEPE et al. 2006).

Forecasting of low visibility and fog is still poor in comparison with the forecasting of precipitation by use of the same models (ZHOU et al. 2011).

The models used in this investigation were: 12 km NAM, 13-km-RUC, and 32 km-WRF-NMM from the National Center for Environmental Prediction (NCEP). Use of the multiple-rule-based fog-detection scheme significantly improves the fog-forecasting ability of all three models compared with visibility-diagnosed fog prediction. Combination of both rule-based fog detection and an ensemble technique has also been suggested (ZHOU and DU 2010).

The Fog Remote Sensing and Modeling (FRAM) Project has been described by GULTEPE et al. (2009). The scientific objectives of the FRAM project are to:

– summarize preliminary results and to characterize all processes from fog formation to dissipation;
– characterize fog microphysics for use in numerical weather prediction model applications;
– improve numerical model simulations and remote sensing applications;
– improve and understand instrument capabilities for detection of fog and fog environments and measurements of associated microphysical variables; and
– integrate observational and model data to improve uncertainties in fog forecasting/nowcasting.

Deep analysis of recent studies on fog formation, development, and decay was presented in the review paper by GULTEPE et al. (2007). Analysis of the observations and development of the forecasting models and remote sensing methods were discussed in detail. In particular, with regard to radiation fog formation, the effects of radiative cooling (length of the night) and of inland advection of moist marine air during the previous afternoon were emphasized. With regard to 1D model simulations, the authors concluded that the development of fog is mainly driven by the atmospheric radiation field, turbulent mixing, and the fluxes of moisture and heat at the Earth's surface. Other dynamic processes, for example horizontal advection or large-scale subsidence, are usually not considered.

Moreover, the research on fog climatology reported by GULTEPE et al. (2007) reveals significant advances in some regions of the world, for example Halifax, Nova Scotia, but little evidence of study of fog in the tropical regions. The study of fog in these regions can be used as a basis for the identification of important climatological conditions.

A parameterized fog (PAFOG) forecasting model has been developed by BOTT and TRAUTMANN (2002) for radiation fog and low-level stratiform clouds in Germany. The high-resolution regional model MM5 and the PAFOG model were used for analysis and forecasting of intense fog (FEDOROVA et al. 2013). Fog formation was simulated by the PAFOG model and satisfactory results were obtained for 10 h antecedence. The authors of the PAFOG model provided it for use for fog forecasting in Maceio, which is located in the tropical region. Although the general conditions in Europe and in the tropical region of Maceio are different, the absence of frontal zones during radiation fog in Europe during all events in Maceio, and the location of all fog incidents inside the air mass, were somewhat similar for both sets of conditions.

The first objective of the work discussed in this paper was to analyze all fog events during five years in the tropical region of the Brazilian northeast (BNE) and to characterize all processes from fog formation to dissipation, including description of:

– in-situ observations;
– synoptic conditions;
– thermodynamic processes; and
– the relationship with sea surface temperature (SST).

The second objective was application of input data (from surface meteorological stations and the

WRF model) from the 1D PAFOG model in all cases whenever possible during the study period in Maceio.

Because the PAFOG model was developed for Germany, where the vegetation is very different than that on the northern coast of Brazil, the third objective was to study the effect of vegetation on fog at Maceio Airport by use of the PAFOG model. This study can, according to GULTEPE et al. (2007), help the development of better understanding of fog formation and of forecasting methods for the tropical region.

In the next section, a brief description of the data sources, models, and methods used will be given. In the "Results" section we first describe analysis of synoptic and thermodynamic processes for all fog events during the five years studied. We then discuss the relationship of fog events with SST distribution and anomalies, and testing of the PAFOG model for short-term fog forecasting. Initial testing with the basic initial variables was tested using the vegetation conditions for Maceio airport. The main conclusions of the study are summarized in the section "Conclusions".

2. Data Source and Methodology

Fog occurrence at Maceio airport (9°31′S and 35°47′W; Fig. 1) during the five years 2002–2005 and 2007 has already been studied by FEDOROVA et al. (2013), who identified eight fog events, although only one was studied in detail. In this paper were present results from study of all the fog events during these years. Fog was recorded in April (1 event), May (1 event), June (2 events) and July (4 events) of the years mentioned above (eight fog events in total, Table 1). Data from the meteorological station at the Maceio Airport were used for analysis of meteorological variables on a foggy day and two days before the event.

2.1. Analysis of Synoptic and Thermodynamic Processes

All fog events were studied by use of hourly data from the surface weather station at Maceio airport, the re-analysis data from the NCEP, the European

Centre for Medium-Range Weather Forecast (ECMWF), and the Weather Research and Forecasting (WRF) high-resolution regional model. Satellite infrared images were obtained from the website of the National Oceanic and Atmospheric Administration (NOAA): http://www.cdc.noaa.gov. The website http://www.ecmwf.int was used to obtain ECMWF data with horizontal resolution 0.75° × 0.75°. WRF information with 0.18° × 0.18° resolution was supplied by the Laboratory for Atmospheric Modeling of the Institute of Atmospheric Science at the Federal University of Alagoas.

The synoptic conditions that prevailed before and during fog events were studied by using different re-analysis products of NCEP. Firstly, the existence and location of the main systems, for example the intertropical convergence zone, frontal zones, and upper tropospheric cyclonic vortex were analyzed by use of infrared satellite imagery and streamline maps at low (925 hPa), middle (500 hPa), and high (200 hPa) levels. Air current distribution at low, middle, and high levels was then analyzed in the study region. This was done because a previous study (FEDOROVA et al. 2008) showed fog formation in a trough near the surface (WDTW). Temperature and moisture advection were also used for analysis of the fog formation processes in the study region.

Temperature and humidity vertical profiles and, also, vertical velocity profiles were elaborated by NCEP/DOE II, ECMWF, and WRF models. Results of the vertical velocity calculations were compared for the different models, because of the absence of any observational methods at the meteorological stations.

The relationship between fog formation and SST was also studied. Daily average SSTs were obtained from the National Environmental Satellite, Data and Information Service (NESDIS) by using the National Climatic Data Center (NCDC) website: http://www.ncdc.noaa.gov. SST values near the coast of Maceio were used. The airport in Maceio is located 20 km from the coast (Fig. 1).

2.2. Fog Forecast Using the PAFOG Model

The dynamic part of PAFOG is a 1D model of the atmospheric boundary layer consisting of a set of
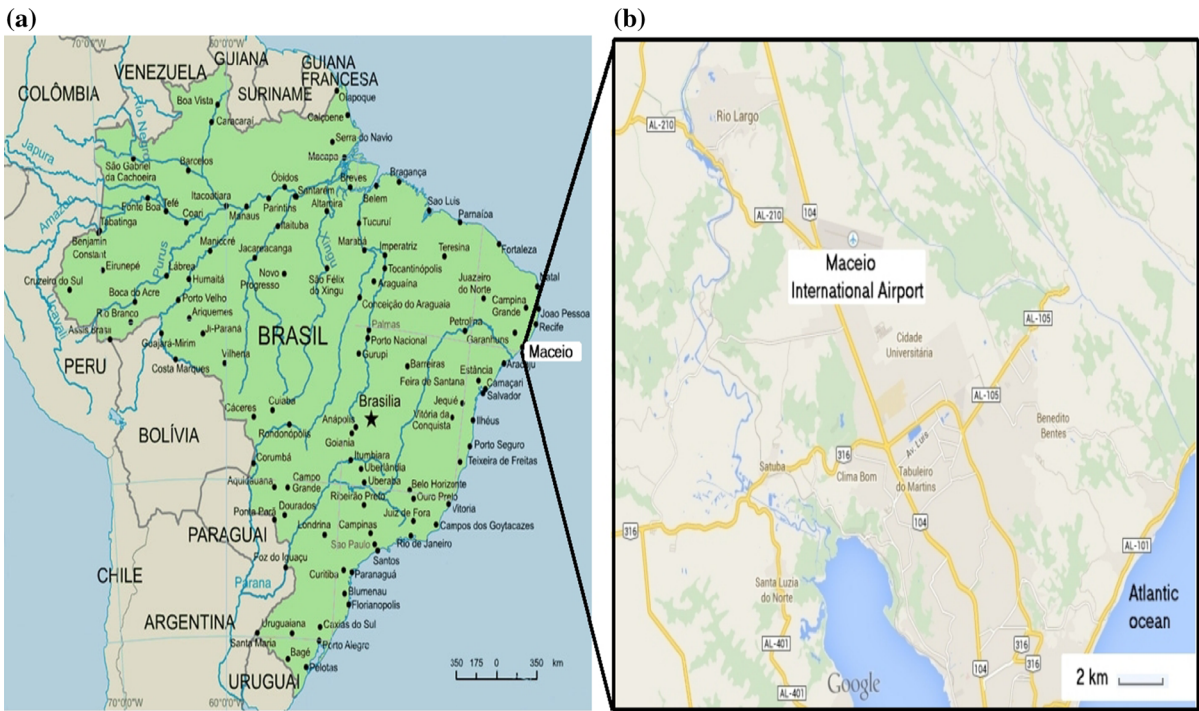
(a)　　　　　　　　　　　　　　　　　　　　**(b)**

Figure 1
Location of: **a** Maceio in Brazil and **b** Maceio airport in relation to the ocean and river

Table 1

Characteristics of fog events and air currents at the main levels

Day	V (m)	D (h)	925 hPa	500 hPa	200 hPa	Div
12/04/2002	700	0.68	C_W/C	C	A	Div_E
11/07/2002	800	0.50	C_E/C	C	A	Div_S
12/07/2002	900	1.00	C_E/C	C	A	Div_S
01/06/2003	500	1.00	C_E/C	A	A	Div_E
02/06/2004	650	0.68	C/A	C	A	–
21/05/2005	300	0.30	C/A	C	A	–
14/07/2005	200	1.91	C/C	A	A	Div_S
26/07/2007	200	3.68	C_E/C	A	A	Div_E

Curvature of the current at the levels 925 (day −1/day of event), 550, and 200 hPa, respectively

E, W, and S show the position relative to the airport of the axis, trough, ridge, and region with Div

V minimum visibility, D fog duration, C cyclonic, A anticyclonic, *Div* divergence of air current

prognostic equations for the horizontal wind field, the potential temperature, and the specific humidity (BOTT *et al.* 1990; SIEBERT *et al.* 1992). Turbulence is treated with the 2.5 level model of MELLOR and YAMADA (1982). Radiation calculations are performed with the y-two stream approximation of ZDUNKOWSKI *et al.* (1982). Soil is treated as a porous medium consisting of dry air, water vapor, water, and the soil matrix. The soil type is taken as sandy loam. The uptake of water by roots is calculated by assuming that the water flow into the roots balances the loss of water as a result of evapotranspiration by the plants.

The 1D PAFOG model of the atmospheric boundary layer consists of four modules:

1. dynamics;
2. microphysics;
3. radiation; and
4. low vegetation (BOTT and TRAUTMANN 2002).

Module 1: geographical data (latitude, longitude and altitude of the meteorological station); ground (ground type); vegetation (height and covering); meteorological station data (pressure; air and dew point temperatures, and relative humidity at 2 m; temperature at the ground; visibility). Module 2: cloudiness at the low, middle, and high levels. Module 3: radiosonde data (pressure; air and dew point temperatures; geostrophic wind velocity; level). Module 4: ground temperature and humidity at different depths. Hourly surface meteorological data from the weather station at the Maceio airport were used as the input data for Modules 1, 2, and 4 of the model. Because of a lack of the radiosonde data in Maceio, WRF model data were used in Module 3. The PAFOG model was used to forecast fog formation with 24 h antecedence.

2.3. Effect of Vegetation on Fog Formation

The predominant vegetation around Maceio Airport is fast-growing sugarcane. Fog events were registered in different months from April to July. Sugarcane has different developmental stages during this time period, therefore different vegetation conditions were used for each fog event (Fig. 2).

Eight variables were used in the paper by BOTT and TRAUTMANN (2002) for the region in Germany (in the text below it is called Germany). On the basis of previous studies (ROBERTSON et al. 1999; ALMEIDA et al. 2008; SANTOS et al. 2008; FERREIRA JUNIOR et al. 2012), the eight vegetation conditions used in the simulations were modified for the tropical region.

1. The canopy height is much greater than in Germany (0.15 m) and is usually 0.6–1 m in April, up to 2 m in May, reaching 4 m in June.
2. The shielding factor is similar to that in Germany (0.8) and varies, usually between 0.5 and 0.7 in April, reaching 0.8 during other months.
3. The leaf area index grows from April to July: 1–3 in April, 2–4 in May, and 3–5 in June and July. This number in Germany is usually 4.

4. The albedo of the foliage is also similar (0.16–0.20) to that in Germany (0.20).
5. The maximum water storage of foliage is much greater than in Germany (0.50) and varies from 1 to 5 kg/m^2.
6. The minimum stomata resistance varied from 70 to 200 s/m during all the study periods and is similar to the number typically used in Germany (200 s/m).
7. The seasonal growing factor is 0–1 in April and May, increasing to 2 in June and to 3 in July. It is 3 in Germany.
8. The albedo of the earth's surface is the same, 0.20–0.25 (0.25 in Germany).

Comparison of the vegetation conditions in Germany and on the Northern Coast of Brazil reveals a substantial difference for the 1st and 5th vegetation conditions listed above and a slight difference for the 2nd and 3rd conditions, which vary every month.

3. Results

Fog duration varied from 20 min to 4 h and its intensity was weak or moderate (Table 1). It is interesting to note that wind direction was from the continent toward the ocean (a night breeze) during minimum visibility for all events.

3.1. Analysis of the Meteorological Variables for Fog Days

Analysis of clouds observed at the meteorological station during fog days reveals an association of this phenomenon with cumulus and altocumulus for all fog events. Mist was detected at the meteorological station before fog formation in events without rain. For example, Fig. 3b shows mist occurrence at approximately 00 h, before the fog. After fog events, lifted fog caused the formation of stratus clouds, which were identified for six events.

Temperature and pressure have a typical daily variation for all fog events (Fig. 3b). A daily pressure variation of approximately 3 hPa is typical for this region. It is associated with trough formation at the low level because of daily heating (RODRIGUES et al.
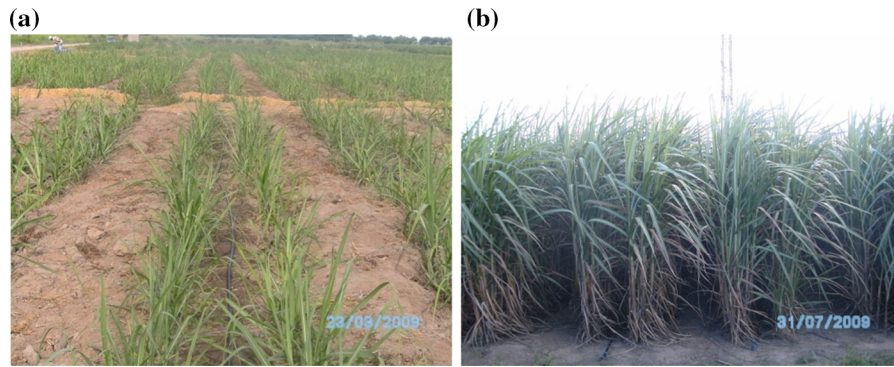
Figure 2
Fast-growing sugarcane around the Maceio Airport during different developmental stages: **a** initial stage (23/03/2009) and **b** crop development stage (31/07/2009)

2010). Also, observational data revealed weak temperature and pressure variations between fog events: minimum temperature during fog events was between 20.4 and 24.1 °C, and pressure was from 998.6 to 1,004.4 hPa. At the same time, few oscillations of the pressure line coinciding with the fog time were observed. Relative and specific (g/kg) humidity also increased in this period (Fig. 3a–c).

Typical wind speed for radiation fog formation was up to 2 m/s during events; it reached 3 m/s on one occasion only. It is important to note that wind direction changed during fog formation and was from the west, southwest, or northwest (230–300°). Seven fog events were accompanied by this changing wind direction and only one event was calm. Changes in wind direction occurred every day because of a breeze. Moreover, a trade wind is very constant in this region. The trade wind is from southeast, east, or northeast (from the ocean) during whole day. Therefore, the daily wind speed (daily breeze together with the trade wind) from the ocean is higher than the night wind speed from the continent (the night breeze and the trade wind have opposite directions). This time period with a change in wind direction contributes to fog formation. Moreover, the night wind is from a river region to the west of the airport (Fig. 1). Evaporation of the river creates a humid surface layer. Wind from the river region brings this humidity and humidifying surface to the airport. This effect of the river was noted in the analysis of two fog and stratus events in 1996 (SILVEIRA 2003).

Three fog events were observed after precipitation, but no precipitation was observed during fog.

For example, on 11 July 2002, brief rain finished 10 min before fog formation. Evaporation from wet surfaces and raindrops humidify the air. This day was calm, and evaporation from the humid surface and raindrops caused increasing humidity, which was an important and additional mechanism for fog formation.

Cross-sections passing through the airport and the coast show accumulation of humidity at low levels (Fig. 4a, c) up to 900 hPa, approximately. Only for one event, on 26 July 2007, when fog was intense at the airport and Cumulonimbus development was observed over the ocean at a distance of 20 km, was humidity high at levels up to 600–500 hPa (Fig. 4b, d). Specific humidity at Maceio airport was estimated as 16.47 g/kg by the model and 19.4 g/kg from observational data on 12 April 2002 and as 16.01 and 16.0 g/kg, respectively, on 26 July 2007.

The predominant wind direction was from the ocean at all levels. Wind from the continent was at high levels, between 400 and 200 hPa, and at the middle levels, between 800 and 700 hPa, only (Fig. 4a, c). During the fog event on 26 July 2007 wind was direction from the ocean at all levels (Fig. 4b, d). During both events a night breeze from the continent was present at the surface level (up to 85 m) between 35.7° and 36.3°W. This wind is connected with the breeze and trade wind. The trade winds are very intense during the whole year because of the stable position of the subtropical high in the Atlantic. During the day, before a fog event, the daily breeze from the ocean has the same direction as the
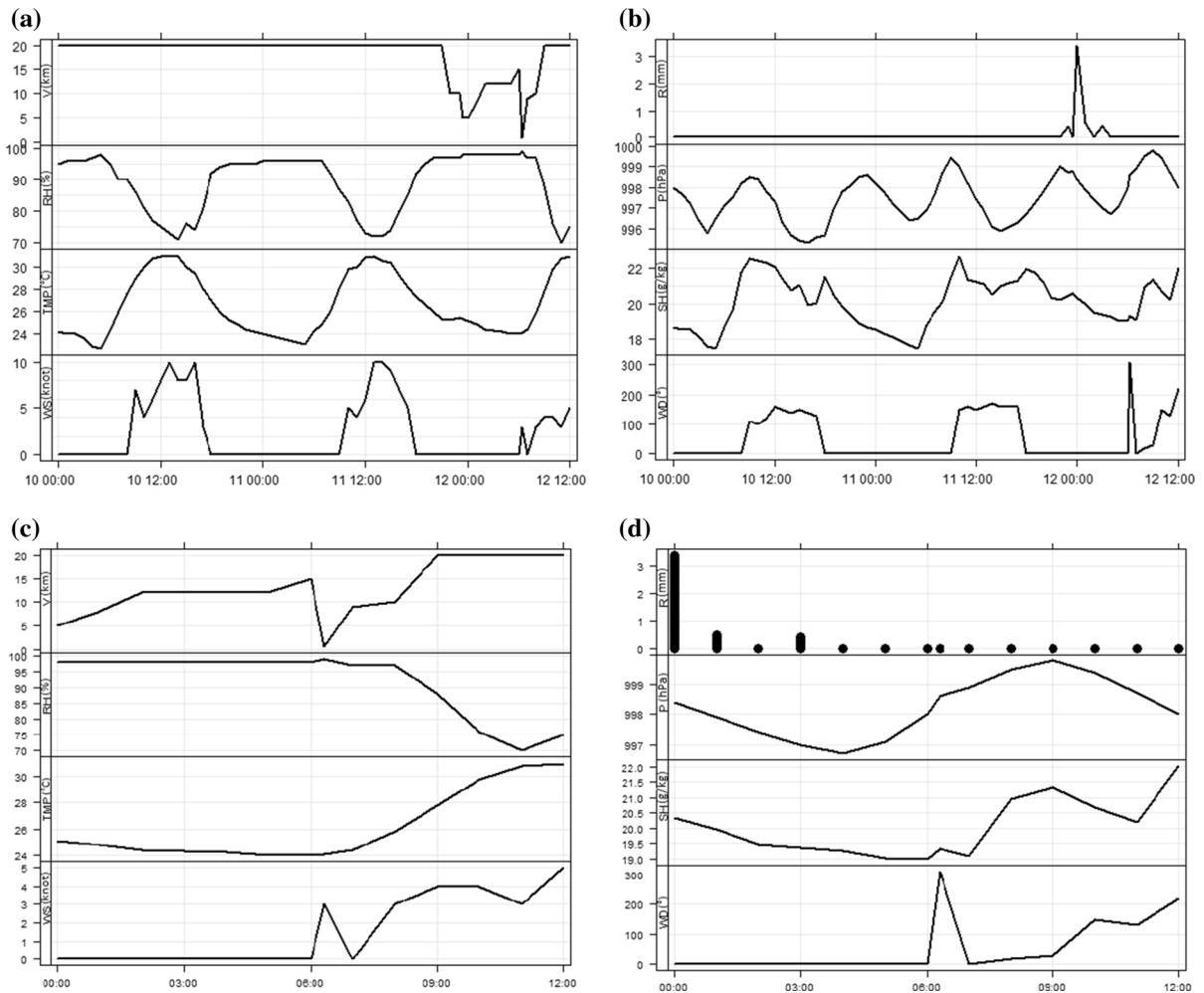
Figure 3
Variation of meteorological variables at the meteorological station at the airport in the time period from 00 h on 10 April 2002 to 12 h on 12 April 2002 (**a** and **b**) and in more detail for the fog night from 00 to 12 h on 12 April 2002 (**c** and **d**). Meteorological variables are: *V* (visibility), *P* (pressure), *R* (rain), *RH* (relative humidity), *TEMP* (temperature), *SH* (specific humidity), *WD* (wind direction), *WS* (wind speed). *h* is local time

trade winds and transports moisture from the ocean. During the night, breezes from the continent were weak, which was confirmed by data from the airport meteorological station. This occurred because the night breeze has a direction opposite to that of the trade wind. At the same time, the direction of the wind during the night was from the river region (Fig. 1). Therefore, high humidity conditions were present before the fog. The temperature subsequently decreased during the night and created conditions for fog formation before sunrise.

3.2. Synoptic Conditions

A synoptic analysis in the tropical region of the BNE usually begins with identification of the principal synoptic scale systems, for example the intertropical convergence zone (ITCZ), the upper tropospheric cyclonic vortex (UTCV), the western periphery of frontal zones (FZ), and easterly waves (EW). These systems are associated with the largest amounts of rain and other adverse phenomena. Identification of these systems is based on analysis of streamline maps at low, middle, and high levels
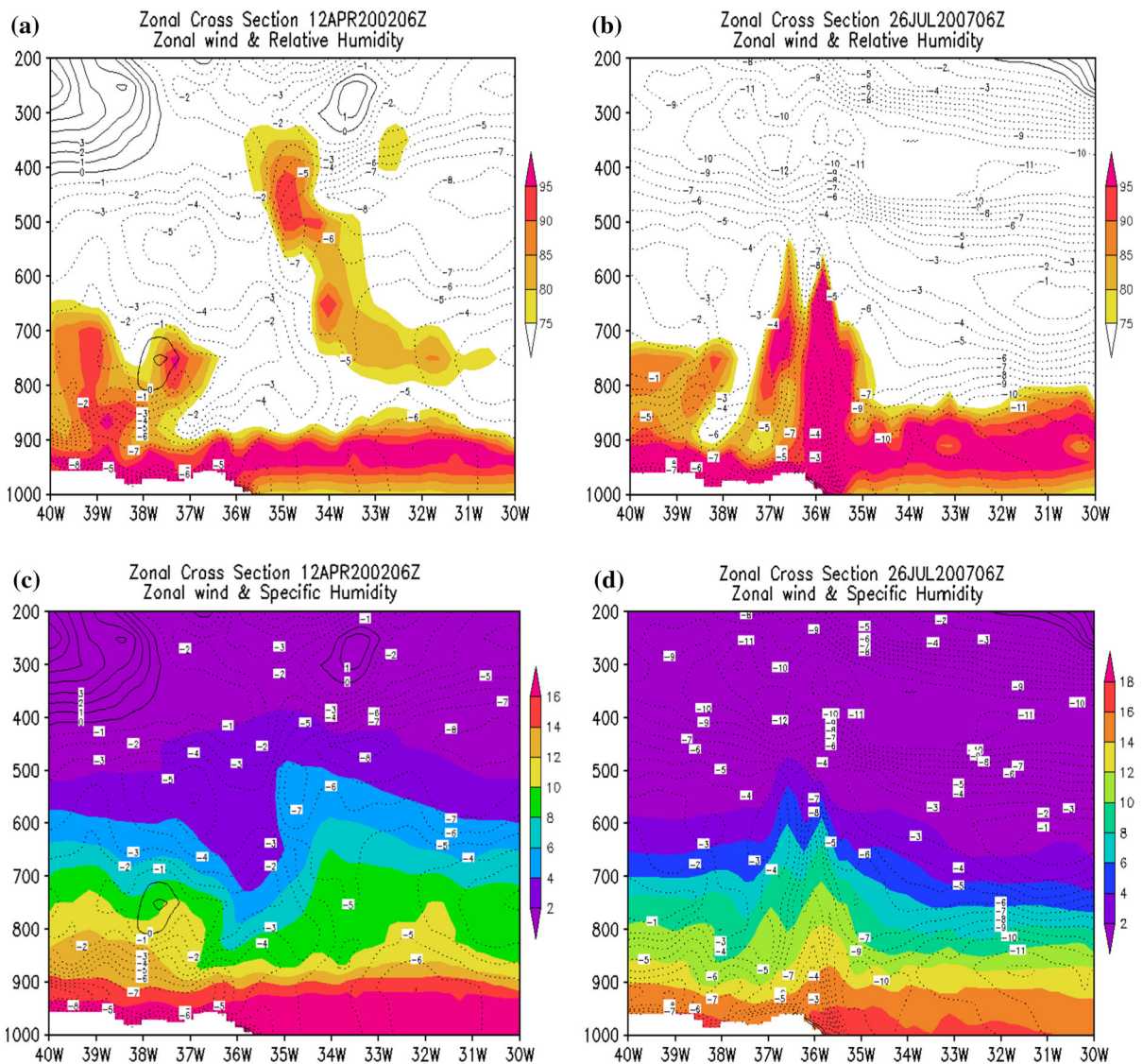
Figure 4

Zonal vertical section by WRF model along 9°31′S, which passes through the airport and coast at 35°47′W: **a** and **b** zonal wind and relative humidity on 12/04/2002 (**a**) and 26/07/2007 (**b**); **c** and **d** zonal wind and specific humidity on 12/04/2002 (**c**) and 26/07/2007 (**d**)

(Vasquez 2000; Kousky 1979; Kousky and Gan 1981). Synoptic analysis shows that ITCZ and FZ were observed far from the BNE during the fog events. Also, the UTCV, which is a typical system in this region, was never identified during fog events. This result especially justifies use of the PAFOG model, because conditions in the tropical region in this case are more similar to the conditions inside an air mass in the extratropical region, which is far from frontal zones.

The absence of these systems from the study region shows that trade winds affected the weather in this region during the study days. Usually, trade winds associated with cumulus cloud at low levels are observed in the study region during the entire year and blow from southeast to northeast. Baric troughs at low levels are rarely formed in this current (Molhon and Bernardo 2002) and are associated with adverse meteorological phenomena (Rodrigues et al. 2010). These baric troughs were denoted

WDTW (MOLHON and BERNARDO 2002). Unfortunately, little information about WDTW in the study region has been published. The method of WDTW identification, described by MOLHON and BERNARDO (2002) includes definition of troughs on streamline maps at low levels and the absence of troughs at middle and high levels. Therefore, this analysis was performed. Trade winds were associated with a subtropical high in the Atlantic near the African coast in all fog events. Some cyclonic or anticyclonic circulation was observed over the study region; therefore, air currents at all levels were studied in detail. Air current distribution at low, middle, and high levels is presented in Table 1.

Fog events were associated with cyclonic curvature (trough) at low levels on six fog days and anticyclonic curvature on two days (Table 1). The trough axis was over the BNE (C in the table) or to the east over the ocean (C_E in the table). The trough was to the west during one event only. Cyclonic curvature at low levels was observed on all previous days. All these troughs were associated with wave disturbances in the trade winds. Cyclonic and anticyclonic curvature was detected at middle levels. Anticyclonic curvature was observed at high levels during all events. These results confirmed previous conclusions (FEDOROVA et al. 2008, 2013) and show that wave disturbances in the trade winds (which are associated with cyclonic curvature of the air current at low levels) is the main system during fog. Also, a divergence of air current was observed during six events. This divergence of air current at low levels was located over the ocean slightly to the east of the BNE for three events and slightly to the south of the BNE for another three events. The absence of divergence occurred solely during two events with anticyclonic curvature of the air current at low levels.

For example, synoptic conditions on 11 July 2002 are presented in Fig. 5. This figure reveals air currents at low and high levels only, because air currents at the middle levels had no typical behavior during fog (Table 1). Intertropical convergence zone and frontal zones were observed far from the BNE along 3°N and 20°S, respectively. The trough axis at low levels was seen over the coastal region of the BNE. The divergence of the air current at low levels

was to the south of the BNE and crossed the Brazilian coast between 10° and 20°S, approximately. The ridge with anticyclonic curvature of the air current was identified over the BNE at high levels (200 hPa).

Temperature advection was identical during all fog events and was weak (from $0–5 \times 10^{-5}$ °C/s) (Fig. 6a). Humidity advection was also weak in all events (between 0 and -5×10^{-5}, g/kg s) (Fig. 6b). Weak temperature and humidity advection also confirm the absence of the frontal zones in the study region. However, a humidity confluence was observed during all fog events. This confluence was located along the ocean coast and reached its maximum value (-0.00045 g/kg s) on 14 July 2005 (Fig. 6c). A humidity confluence is an important factor in fog formation.

The absence of the intertropical convergence zone and frontal zones in the study region result in general conditions similar to those for radiation fog formation and, therefore, make possible use of the PAFOG model. However, it is necessary to emphasize that classic radiation fog is formed inside the extratropical high. These systems were not observed in the tropical region of the BNE. Fog in the BNE was associated with troughs connected with wave disturbances in the trade winds. Other conditions, for example low wind velocity, decreases in air temperature during the night, low temperature, and humidity advection, were similar to those required for radiation fog formation.

Summarizing the results given above, it is possible to make the following conclusion regarding the synoptic conditions for fog formation in the tropical region of the BNE. Cyclonic curvature at low levels was detected on the day before all fog events, was predominant (six events) during the fog days, and was associated with wave disturbances in the trade winds (WDTW). The divergence of the air current at low levels was located near the coast over the ocean to the east or south of the BNE during all events with cyclonic curvature. Anticyclonic curvature at high levels was observed during all fog events. During the fog events, wind was from the continent. Air currents at low levels create conditions for confluence of humidity, which is an important factor for fog formation.
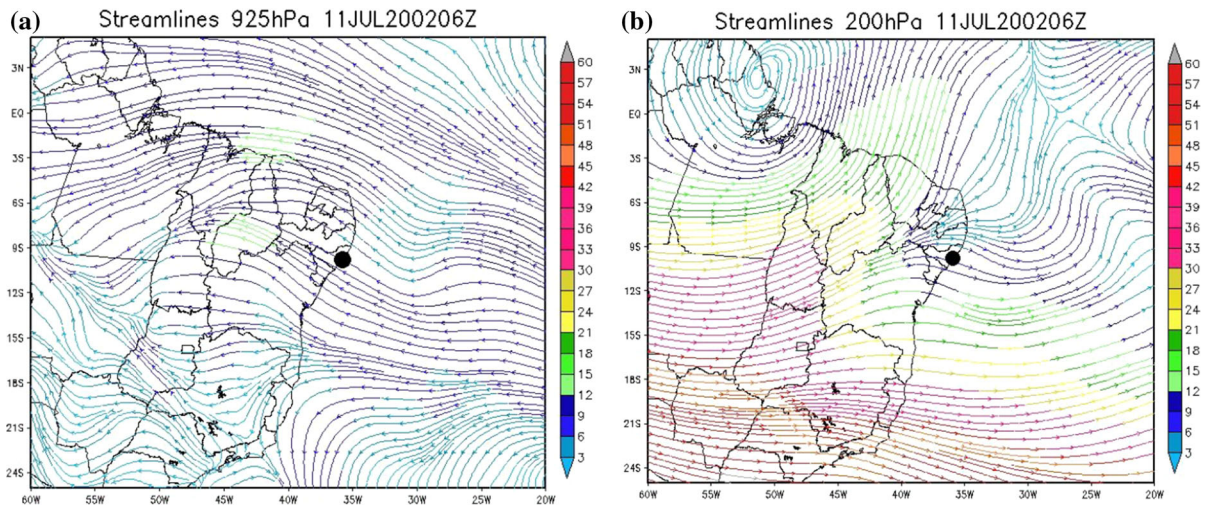
Figure 5
Stream lines at levels 925 hPa (**a**) and 200 hPa (**b**) at 06UTC on 11/07/2002. The *color* shows wind speed. The *point* shows the location of Maceio city

3.3. *Thermodynamic Analysis*

Vertical profiles of NCEP/DOE II reveal instability of conditions at low levels (1,000–850 hPa) and a quite humid layer with variation of differences between temperature and dew point temperature (T − Td) between 1 and 5 °C. A dry and stable level was observed above. Examples for two days are presented in Figs. 7 and 8.

The vertical profile of the ECMWF model reveals a thinner layer of unstable conditions than that of the NCEP/DOE II model, up to 900 hPa, on average. The humidity at this layer was higher (T − Td <3 °C). An absence of thermal inversion at the low levels was identified by the NCEP/DOE II and ECMWF models (Figs. 7, 8).

The temperature profile predicted by the WRF model reveals the best conditions for fog formation in comparison with the other models. A typical temperature profile during fog events obtained by use of the WRF model has the following characteristics:

1. temperature inversion from the surface up to 166 m (985 hPa);
2. a humid layer (T − Td varying from 0.3 to 1.6 °C) up to the top of inversion;
3. the existence of unstable conditions above the inversion layer between 985 and 860 hPa; an
4. a dry (T − Td varying from 10 to 30 °C) and stable layer above 860 hPa.

A very thin inversion layer was observed in all the temperature profiles of the WRF model. The humid layer above the thermal inversion was of different thickness. A typical layer is presented in Fig. 7c; the layer of maximum humidity of thickness up to 600 hPa is visible in Fig. 8c.

Previous studies (GOMES *et al.* 2011; FEDOROVA *et al.* 2013) have shown that weak lifting at low levels is typical for this tropical region during stratus and fog events. However, sinking is associated with classic radiation fog. Vertical velocity in the study region was atypical for radiation fog formation and, therefore, was analyzed in detail by use of different models. Vertical profiles show predominance of weak (positive or negative) vertical motion up to 0.03 m/s; lifting reached 1.2 m/s at the 700 hPa level only on 1 day, 26 July 2007. The description of this event (FEDOROVA *et al.* 2013) shows very atypical conditions for fog formation in which cumulonimbus was observed at a distance of 20 km from the fog. Therefore, this lifting reflects convection development. Lifting (up to 800–700 hPa, approximately) was observed at the low levels by the NCEP/DOE II and ECMWF models for all events. The WRF model also shows lifting, but two events have sinking to the surface from the 850 and 600 hPa levels. Usually, lifting destroys the inversion layer and does not create conditions for fog formation. Vertical motion at the middle levels were different for each model
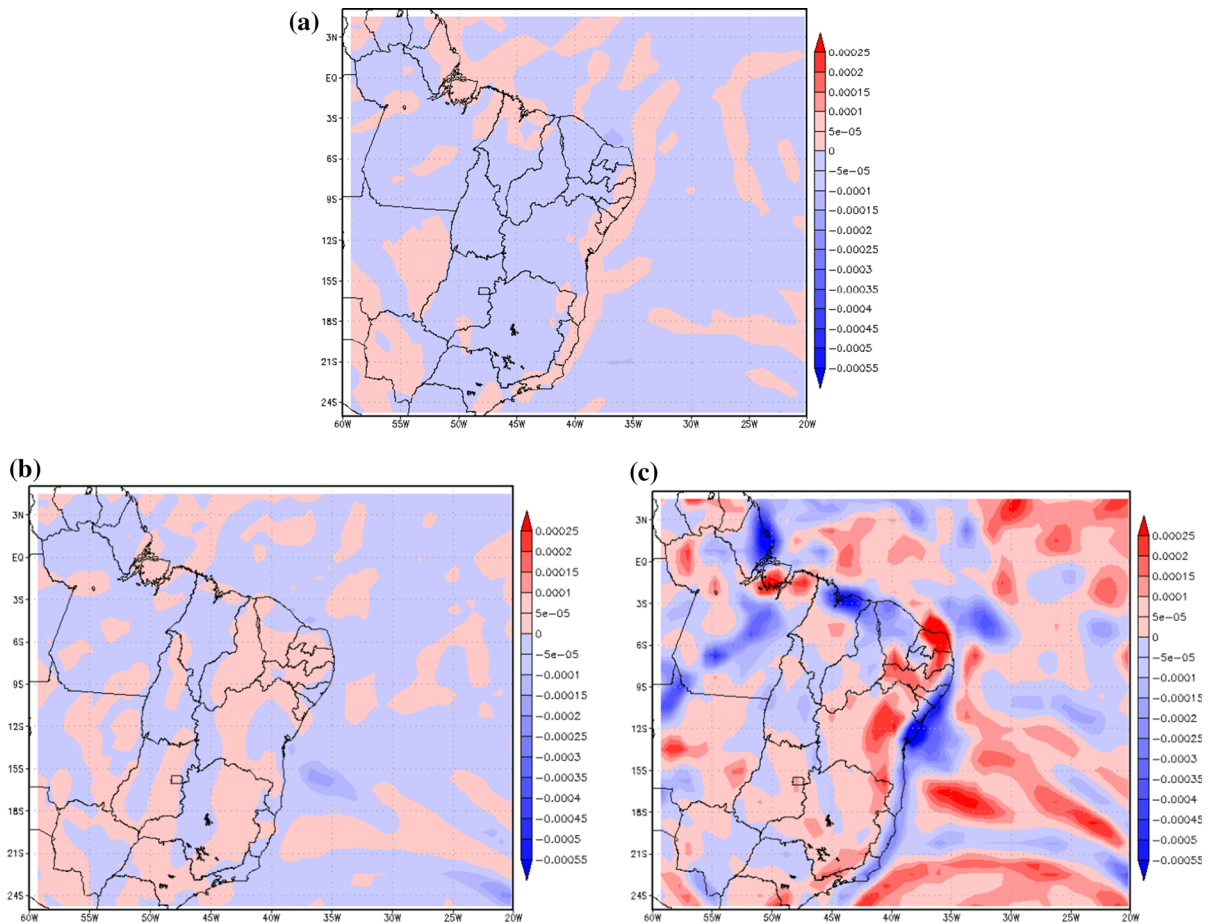
(a)

(b)   **(c)**

Figure 6

Temperature advection (°C/s) (**a**), humidity advection (g/kg s) (**b**), and divergence of humidity (g/kg s) (**c**) at the 1,000 hPa level, from ECMWF data on 14 July 2005

used: sinking was observed for five, four and three events by the NCEP/DOE II, WRF, and ECMWF models, respectively. Sinking was predominant at the high levels in the ECMWF and WRF models (in six and seven events, respectively).

The results of these models reveal differences in the vertical motion calculations. In the authors' opinion, this is related to a different horizontal resolution and noise of the models. Cumulus and altocumulus clouds were observed during fog event days (discussed in the section "Analysis of the Meteorological Variables for Fog Days"). These types of cloud are associated with substantial horizontal variability of vertical motion. For example, a cumulus cloud has both sinking and lifting at distances of kilometers (DJURIC 1994). Therefore,

horizontal resolution of the models used (discussed in the section "Analysis of Synoptic and Thermodynamic Processes") reveals differences in vertical motion calculation. That said, some vertical motion is observed for all events, with the existence of weak lifting at low levels. However, the presence of weak lifting at low levels corresponds to synoptic scale systems (troughs associated with the wave disturbances in the trade winds) identified in the study region.

For example, Fig. 9 shows vertical velocity at Maceio airport at 06UTC on 12 April 2002 and 26 July 2007 according to the NCEP/DOE II, ECMWF, and WRF models. Lifting was observed on 12 April 2002 at low levels by the NCEP/DOE II and ECMWF models. At the same time, the WRF model showed
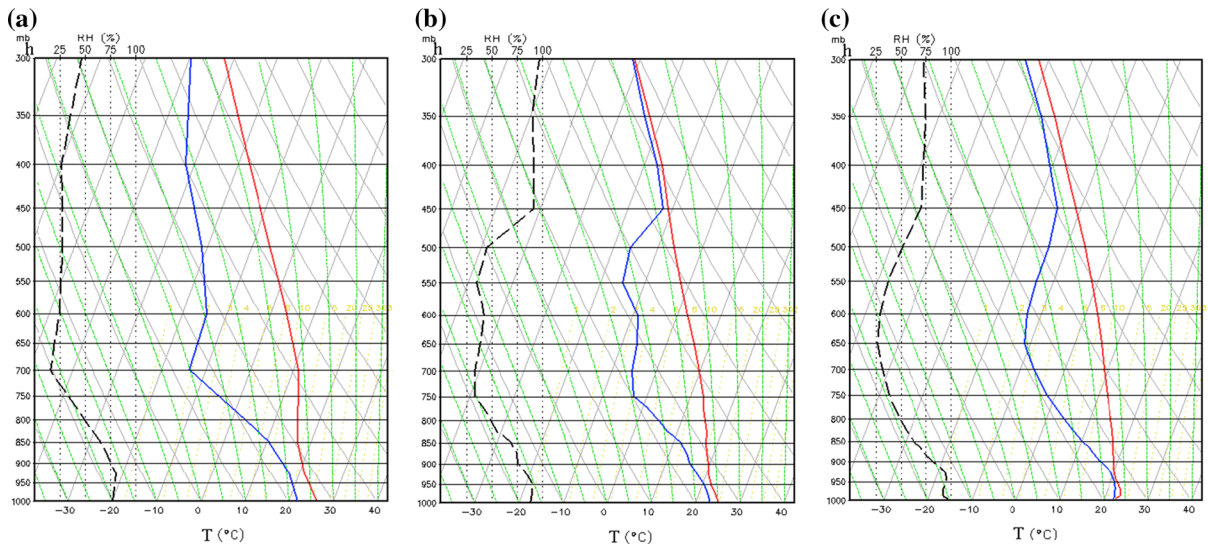
Figure 7
Temperature and humidity vertical profiles at 06UTC on 12 April 2002: by NCEP/DOE II model (**a**), by ECMWF model (**b**), and by WRF model (**c**). The *curves* show vertical distribution of temperature (*solid red line* on right), dew point temperature (*solid blue line* on left) and relative humidity (*dotted line*)
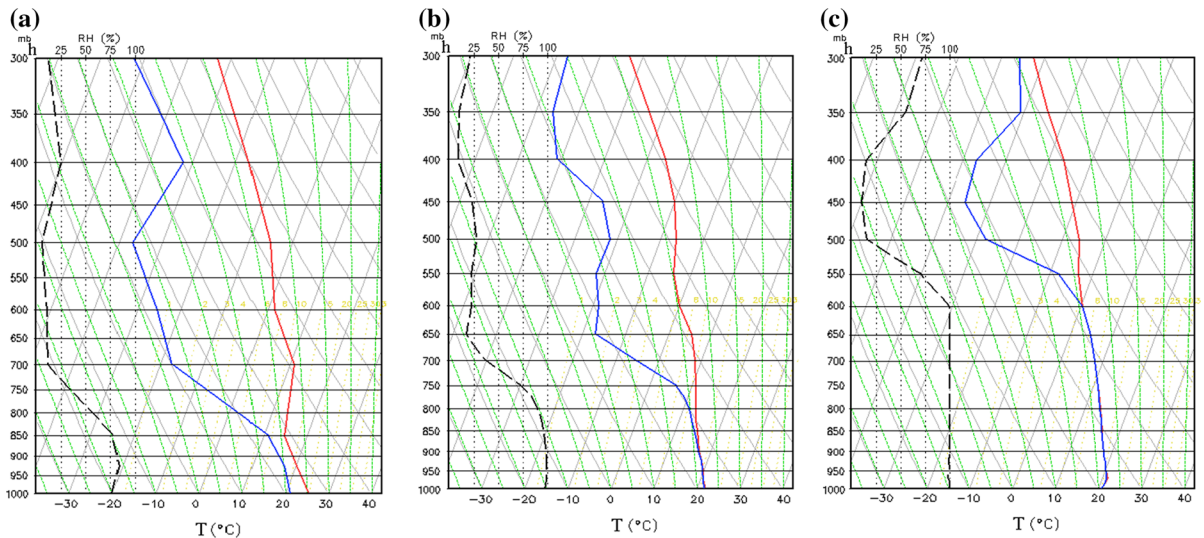

Figure 8
Temperature and humidity vertical profiles at 06UTC on 26 July 2007: by NCEP/DOE II model (**a**), by ECMWF model (**b**), and by WRF model (**c**). The *curves* are the same as in Fig. 3

sinking up to 850 hPa (Fig. 9a). Sinking at high levels was detected by the NCEP/DOE II and ECMWF models, but the WRF model detected sinking at up to 350 hPa. Lifting in the very thin layer (up to 990 hPa) was observed by the NCEP/DOE II model on 26 July 2007 (Fig. 9b). Above this level, this model shows sinking up to 720 hPa and

lifting in the rest of the troposphere. Lifting in the entire troposphere was identified by the ECMWF and WRF models (Fig. 9b, c).

Air mass lifting is because of the confluence of air ((discussed in the section "Synoptic Conditions"). Confluence in the troughs led to humidity accumulation and an increase in the saturated layer.
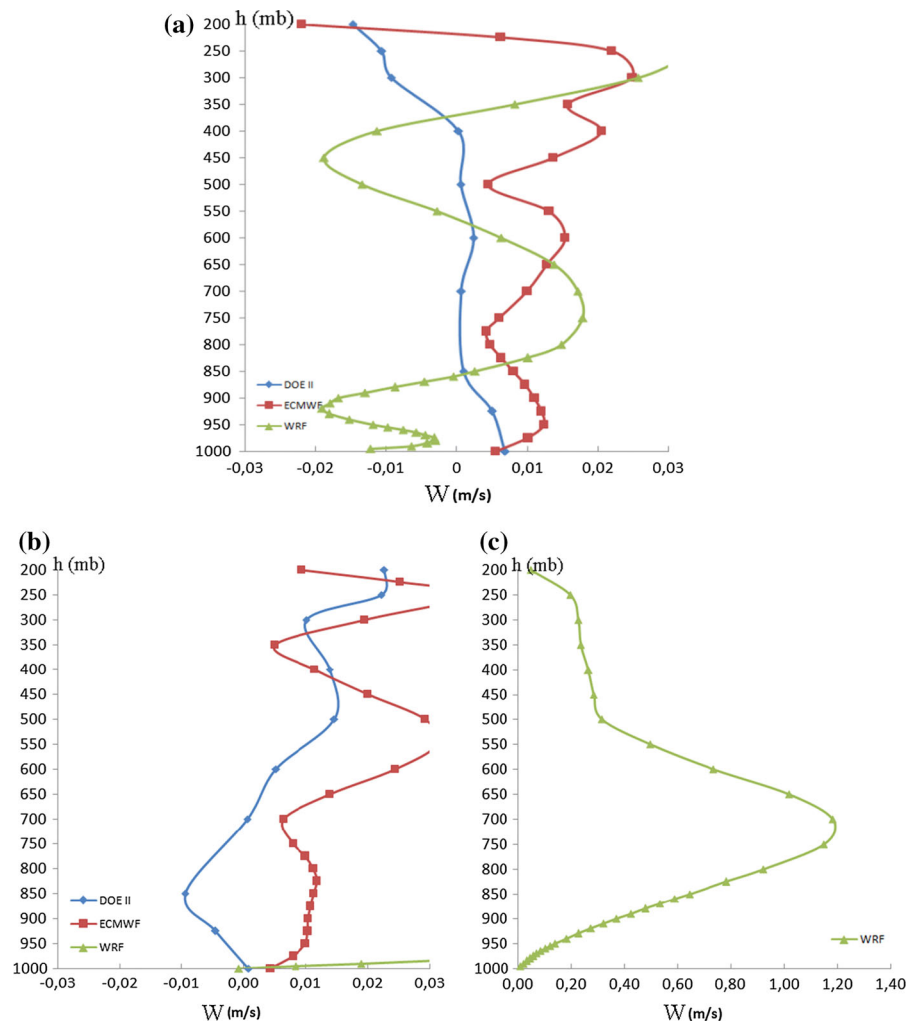
Figure 9

Vertical velocity (m/s) at Maceio airport at 06UTC on 12 April 2002 (**a**) and 26 July 2007 (**b** and **c**) from the NCEP/DOE II model (*blue*), the ECMWF model (*red*), and the WRF model (*green*)

According to Zhou and Ferrier's theory (2008), a deeper saturated or fog layer has a larger critical turbulence threshold that can withstand greater turbulence. So, deepening of the saturated layer because of moist air mass confluence provides a favorable environment for fog formation and persistence.

Summarizing the results reported above, it is possible to make the following conclusion regarding the thermodynamic processes of fog formation in the tropical region of the BNE. Vertical profiles of T and Td reveal weak lifting at low levels in all events in all models and a predominance of sinking at higher levels in the ECMWF and WRF models. The

existence of weak lifting at low levels corresponds to the synoptic scale system (WDTW) identified in the study region. This vertical motion is atypical for radiation fog formation, which is usually associated with sinking in the extratropical high. Weak lifting at low levels is a distinctive condition for fog formation in the tropical region, different from the conditions of a typical radiation fog.

Absence of thermal inversion and conditional instability at low levels were identified by the NCEP/DOE II and ECMWF models up to 850 and 900 hPa, respectively. A typical temperature profile during fog given by the WRF model reveals three layers:

1. a very thin layer (up to 166 m, 985 hPa) of temperature inversion, with a very high humidity (T − Td between 0.3 and 1.6 °C);
2. a conditional instability layer from 985–860 hPa; and
3. a dry and stable layer above 860 hPa.

3.4. Relationship of Fog Events with Sea Surface Temperature

The SST and variation of the SST (VSST) were studied for fog days and two previous days (Table 2). Variation of the SST during the two days before the fog was from 0.18 to 0.92 °C. These SST variations are connected with weak fog events, with visibility of 700–900 m associated in three events with ocean warming (a temperature increase of 0.4–0.8 °C two days before the fog event). Two moderate fog events with visibility of 200–300 m were observed during ocean cooling (−0.2; −0.3 °C). SST was constant (±0.1 °C) during the two events with visibility of 200 and 650 m, respectively. STT increased (0.5 °C) and then decreased (−0.3 °C) in the fog event with visibility of 500 m.

An increase of negative VSST (ocean cooling) during the two days before the fog day was observed for two moderate fog events (with visibility of 200 m). Also, ocean cooling with a decrease of positive VSST was detected for the event with visibility of 300 m. Ocean warming (decrease of the negative VSST and increase of the positive anomaly) was observed during five moderate events. Ocean cooling promotes air temperature decreases near the coast and ocean warming helps to increase humidity in the coastal region.

A comparison of air temperature at the airport (Ta) with SST is presented in Table 3. SST was, on average, higher than the daily average Ta by 3.9 °C during all fog events. Differences between maximum Ta on the fog day and SST were 0.7–1.9 °C for five events; there was a negative difference (−0.9; −0.3 °C) for two events and the difference reached 3.5 °C for one event. The above mentioned difference for the previous day was 0.5–1.1 °C for six events and reached −2.4 and 2.7 for days 11/07/2002 and 02/06/2004. The reduction of the Ta on these previous days was because of continuous cloudiness during all the days, which has rarely been observed in this tropical region (GOMES et al. 2011). The difference between minimum fog night Ta and SST on a fog day was positive for all fog events, with variation from 3.9 up to 6.8 °C. All data show that SST for all fog events was higher than the minimum air temperature during the fog-formation period, in contrast with the typical advection sea fog when the warm and moist air from the land moved over the colder sea surface.

Maps of the SST distribution show one type of warm thermic anomaly near the eastern coast of the BNE (Fig. 10)—a warm oscillation on the sea surface from the equatorial region (Q_N). It is important to note that only a warm oscillation on the sea surface was observed for all fog events (Table 3). A warm sea surface promotes greater air humidity at low

Table 2

Sea surface temperature (SST, °C) and variation of SST (VSST, °C) for the fog day (0) and previous days (−1 and −2) and also SST variation from −2 to fog day (Δ)

Day	SST				VSST		
	−2	−1	0	Δ	−2	−1	0
12/04/2002	28.8	29.0	29.2	0.4	0.58	0.74	0.97
11/07/2002	25.7	26.0	26.4	0.7	0.92	0.63	0.20
12/07/2002	26.0	26.4	26.8	0.8	0.63	0.20	0.28
01/06/2003	27.9	28.4	28.1	0.5/−0.3	0.36	0.85	0.62
02/06/2004	27.4	27.3	27.4	−0.1/0.1	0.18	0.20	0.07
21/05/2005	28.1	28.0	27.9	−0.2	0.34	0.20	0.10
14/07/2005	26.3	26.2	26.3	−0.1/0.1	0.27	0.37	0.21
26/07/2007	26.0	25.8	25.7	−0.3	0.35	0.62	0.65

Table 3

Comparison of air temperature at the airport with SST

Day	Ta min			Ta max			Ta max$_0$ − SST	Ta max$_{-1}$ − SST	SST − Ta min$_0$	WTA
	−2	−1	0	−2	−1	0				
12/04/2002	22.6	23.0	24.0	31.0	31.0	31.0	0.8	0.8	5.2	Q_N
11/07/2002	21.9	21.6	22.0	29.4	24.0	27.8	1.4	−2.4	4.4	Q_N
12/07/2002	21.6	22.0	21.4	24.0	27.8	27.5	0.7	1.0	5.4	Q_N
01/06/2003	21.6	21.4	21.3	27.8	28.7	28.1	−0.3	0.6	6.8	Q_N
02/06/2004	23.4	23.2	23.5	28.7	24.7	30.9	3.5	−2.7	3.9	Q_N
21/05/2005	21.9	22.8	23.2	27.4	28.3	29.8	1.9	0.4	4.7	Q_N
14/07/2005	21.9	19.4	19.9	27.4	27.5	26.3	1.2	1.1	6.4	Q_N
26/07/2007	19.2	19.7	20.6	26.2	24.8	25.7	−0.9	0.5	5.1	Q_N

Minimum and maximum air temperature at the airport (Ta min and Ta max, respectively) for a fog day (0) and previous days (−1 and −2) and differences between air temperature and average sea surface temperature of a fog day (SST$_0$); also the existence of a warm thermic anomaly (WTA) of SST (where S and N show the anomaly from N or from S)
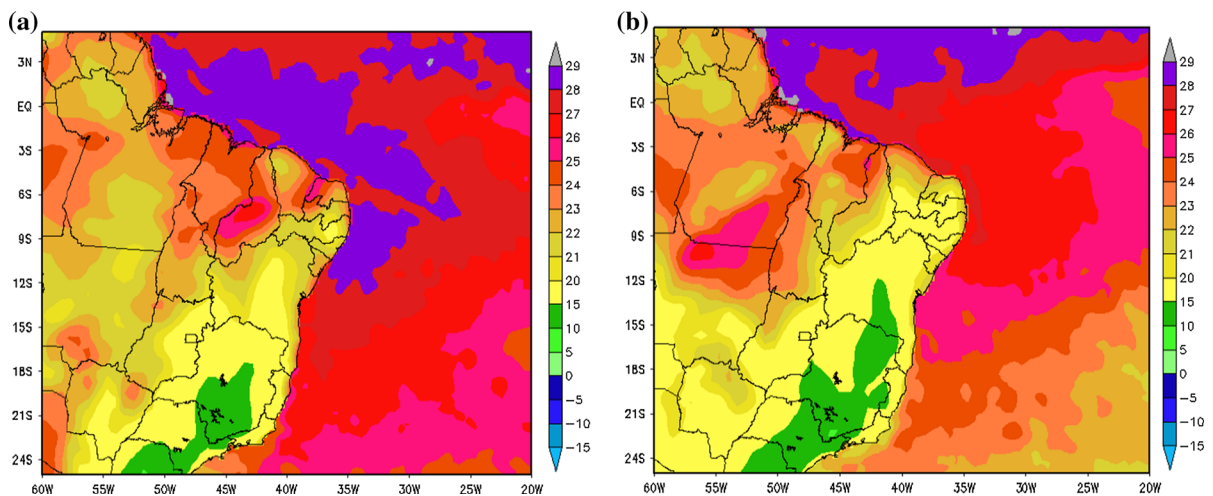

Figure 10
SST distribution near the eastern coast of the BNE on 01/06/2003 (**a**) and 14/07/2005 (**b**)

levels near the coast and also humidity transfer inside the continent, together with a daily breeze on the day before fog formation.

Latent heat flux reached approximately 60–100 W/m^2 in the coastal regions and adjacent ocean. Much of this heat was concentrated near Maceio over the ocean (Fig. 11a) or was observed along the coast (Fig. 11b). Positive latent heat flux indicates humidity evaporation from the surface and, therefore, reveals an increase in the air humidity. For this reason, humidity is more concentrated in the air in this coastal region.

Sensible heat flux maps show Maceio's location between weak negative (down to −10 W/m^2) values

over the continental region and weak positive values (up to 10 W/m^2) over the ocean (Fig. 12a). More significant variations of the sensible heat flux between continental and ocean regions (from −20 to 20 W/m^2) were detected for three events (Fig. 12b). Negative values of the sensible heat flux contribute to air cooling, possible water vapor condensation, and, therefore, fog formation.

Summarizing the results reported above, it is possible to make the following conclusions regarding the effect of the SST on fog formation in the tropical region of the BNE. The SST during nights with fog was approximately 4–7 °C higher than the air temperature at the airport. Also, a warm oscillation on the
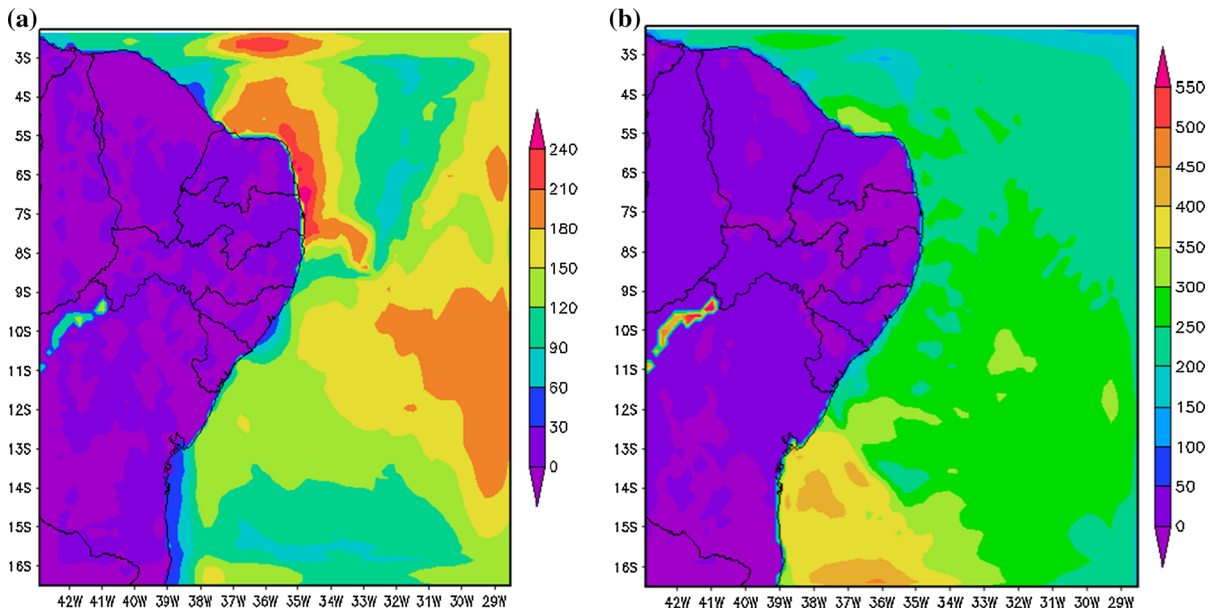
Figure 11
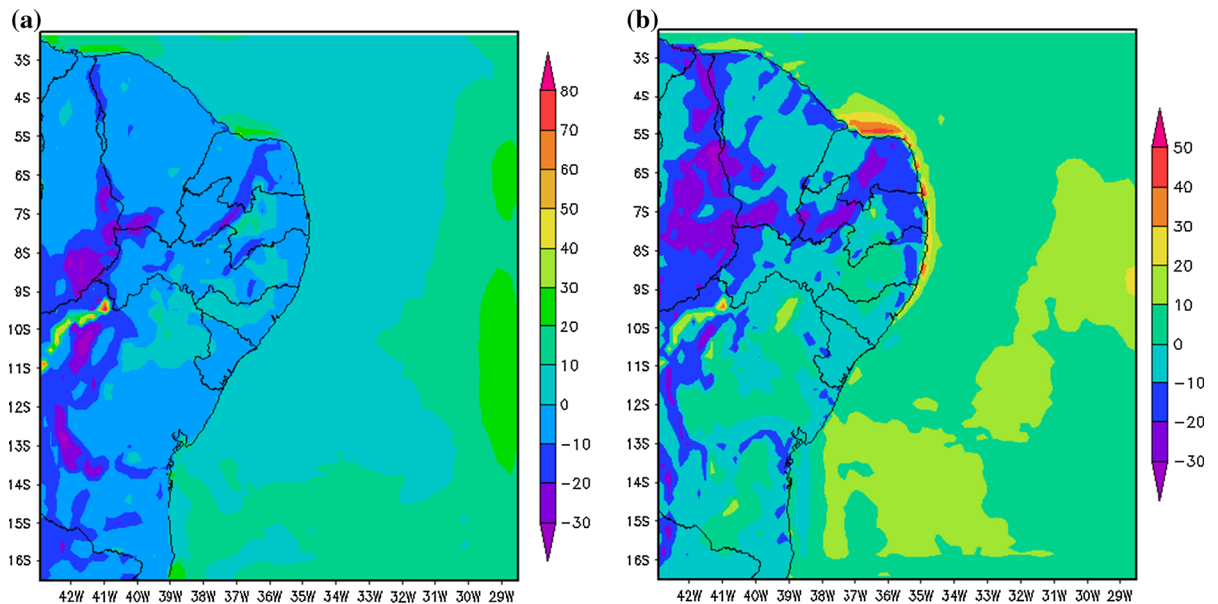Latent heat flux at the surface (W/m²), from WRF data, at 06UTC on 12 Abril 2002 (**a**) and 14 July 2005 (**b**)

Figure 12
Sensible heat flux at the surface (Wm²), from WRF data, at 06UTC on 21 May 2005 (**a**) and 12 July 2002 (**b**)

sea surface near the BNE was observed during all fog events. Very weak temperature and humidity advection was typical for all fog events. All this information shows that conditions for fog formation were contrary to typical conditions for advection sea

fog, when warm air moves over the colder sea surface.

This temperature distribution, in which SST is higher than air temperature, is typical for the type of evaporation of fog formation; air moves from the

continent and fog is formed over the ocean. In this study, however, fog was formed over the continent within 20 km of the coast. Therefore, the studied fog in the tropical region was not the same type as evaporation fog.

Weak, latent heat flux (up to 100 W/m^2) was observed along the coast and, during three events, was concentrated over the ocean near Maceio. Positive latent heat flux is indicative of an increase of air moisture and, therefore, more humidity accumulates in the air in the coastal region. Upward sensible heat flux maps show Maceio's location between weak negative (down to −20 W/m^2) values over the continental region and weak positive values (up to 20 W/m^2) over the ocean. Negative sensible heat flux contributes to air cooling, possible water vapor condensation, and, as a result, fog formation.

3.5. Forecast by the PAFOG Model

3.5.1 Forecast by PAFOG Model with Basic Initial Conditions

The PAFOG model was used for all possible cases. Two fog events (11/07/2002 and 14/07/2005) were observed between rain. Rain during the days before the fog days was recorded for two events (01/06/2003 and 21/05/05). All of these conditions are not favorable for use of the model. Also, the absence of WRF model data prevented use of the model on 02/06/2004. Therefore, the model was used for three events. The forecast was satisfactory for two cases. One event of intense fog on 26 July 2007 has previously been analyzed by FEDOROVA et al. (2013) and was forecast with 9 h antecedence. The forecast visibility was 136 m and the observed visibility was 200 m.

Results for the second fog event are presented in Figs. 13 and 14. Detailed vertical profiles of the temperature and relative humidity before, during, and after the fog event on 12 April 2002, using WRF data, are presented in Fig. 13. A temperature inversion was present from the surface up to 50 m, approximately, before and after the fog event. During the fog (06 local time), the isothermal level was below 50 m and the inversion level was between 50 and 90 m. Relative humidity before the fog event (00 local

time) was 93–98 % below 50 m. During the fog, relative humidity was >95 % below 50 m, approximately 95 % from 50 m to 600 m, 80–95 % from 600 m up to 1300 m.

Fog formation was forecast with 9 h antecedence (line 2, Fig. 14), but the beginning of the fog was predicted with a delay of 3 h. Forecast visibility with 9 and 6 h antecedence was 200 and 120 m, respectively.

The duration of the fog event on 12 July 2002 was 1 h and minimum observational visibility was 900 m. The model shows visibility decreases between 0 and 4 h but the forecasting process was then interrupted. This happens when the results are not consistent. The NCEP/DOE II, ECMWF, and WRF models give different results for humidity at low levels for the fog event on 12 July 2002. The NCEP/DOE II data are indicative of a layer with T − Td between 4 and 5 °C up to 850 hPa; this information did not confirm fog formation. The ECMWF data are indicative of high humidity (T = Td) up to 900 hPa and, therefore, possible fog formation. The WRF vertical profile reveals a very thin humid layer up to 950 hPa. Also, very light rain was observed at 0 h. Other processes were similar to the processes for the other events. This fog event was very weak with a visibility of 900 m, which is near the high limit for fog (1,000 m). Therefore, in the author's opinion, the problem of fog forecasting was the very thin humid layer predicted by WRF model.

All these results show that it is necessary to better understand the conditions of fog development in this tropical region and to continue adaptation of the fog forecast model for this specific region. Integration of specific local observational data with the numerical model in BERGOT et al. (2005) is a good start toward future study development.

3.5.2 Forecast by PAFOG Model with the Vegetation Conditions for Maceio

Low visibility forecasts using vegetation conditions for Germany and the Maceio Airport were compared. Results did not reveal any significant variation of forecast low visibility. Fog was forecast for the same events, and Fig. 15 shows the forecast variation on 12 April 2002 (the same day as discussed in the section
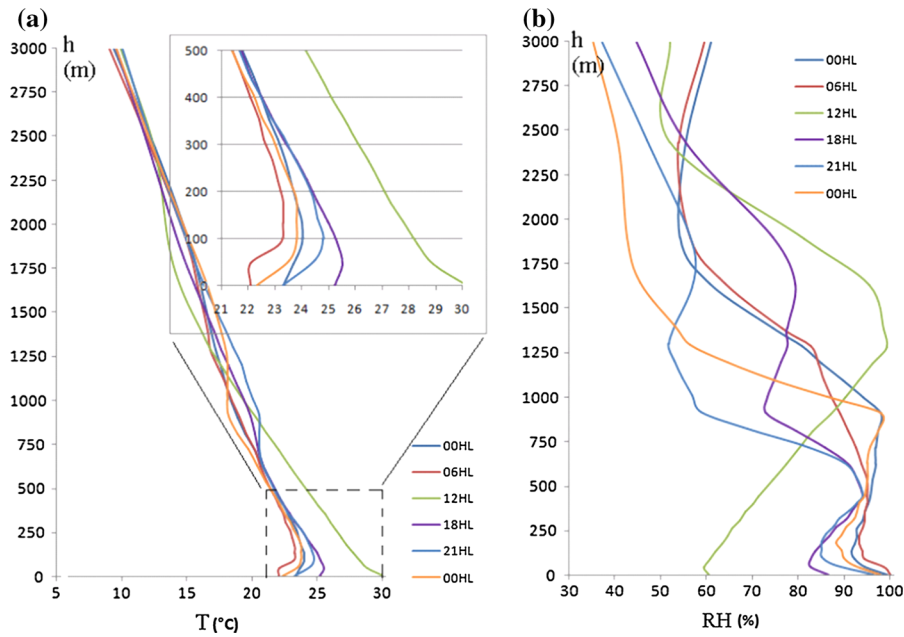
Figure 13
Vertical profiles of the temperature (**a**) and relative humidity (**b**) before, during, and after a fog event on 12 April 2002, using WRF data
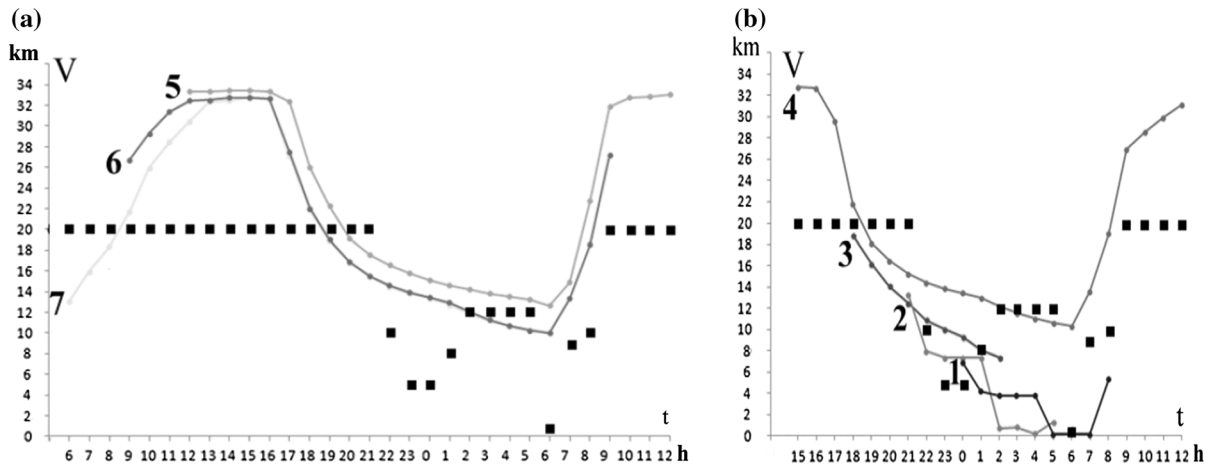

Figure 14
Diagrams of visibility from observational data (*squares*) and according to the PAFOG model forecast (*lines*) 12 April 2002. The forecasts with 24 h (*line 7*), 21 h (*line 6*), and 18 h (*line 5*) antecedence are presented in (**a**) and with 15 h (*line 4*), 12 h (*line 3*), 9 h (*line 2*), and 6 h (*line 1*) antecedence in (**b**). V visibility, t hours during the fog day and during the day before the fog day

"Forecast by PAFOG Model with Basic Initial Conditions" and Fig. 14). Table 4 shows the effect of each vegetation condition on the forecast result. The minimum visibility (observational data) was 700 m on 12 April 2002. Forecast visibility using standard PAFOG model conditions was 118 m (Table 4). Forecast visibility with use of the different

vegetation conditions was not significantly different and varied between 65 m (with a high limit for the 1st variable) and 278 m (with a high limit for the 5th variable). It was mentioned in the section "Effect of Vegetation on Fog Formation" that the 1st and 5th vegetation variables differ from those of the standard conditions.
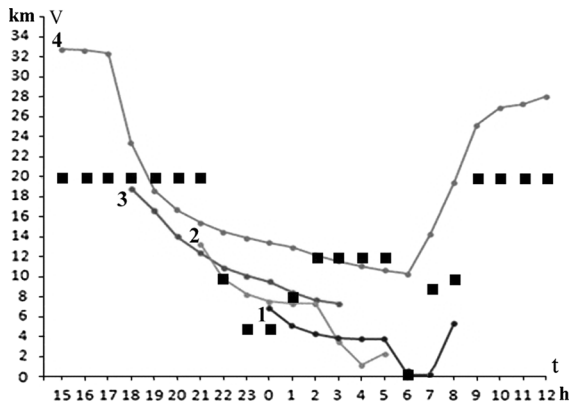
Figure 15

Diagrams of visibility from observational data (*squares*) and forecast by use of the PAFOG model (*lines*) using the Maceio vegetation conditions: 12 April 2002 with 6 h (*line 1*), 9 h (*line 2*), 12 h (*line 3*), and 15 h (*line 4*), antecedence. V visibility, t hours during the fog day and during the day before the fog day

Fog was observed at the meteorological station for 0.68 h and fog duration predicted by use of the standard model substantially was 3 h. With use of a high limit for the 5th variable, predicted fog duration was 1 h, or more similar to the duration observed. Results show (Fig. 15) that the times of fog initiation and duration were predicted more exactly by using vegetation conditions for Maceio.

Fog was forecast with 6 h antecedence by using standard model conditions. The antecedence was increased to 9 h by using the new vegetation conditions (for example, with a high limit for the 5th variable, Table 4).

4. Conclusion

All eight fog events detected in the Maceio region (tropical region of the BNE) during five years were analyzed. Fog duration was short (nearly 4 h for one event only and less than 2 h for four events) and its intensity was weak or moderate.

Summarizing the results reported above, it is possible to make the following conclusions regarding the processes of fog formation in the tropical region of the BNE. For was associated with a synoptic scale air current in the atmosphere, in the form of WDTW much different from typical synoptic scale processes in this region, for example ITCZ, UTCV, EW, and

FZ. A weak confluence in troughs at low levels (that is in WDTW) contributes to weak pressure lifting, which was observed in the line of pressure variation at the meteorological station. Weak lifting at low levels, revealed by the numerical models, was a result of the WDTW occurrence. This current creates a condition for humidity confluence, which was marked by an increase in humidity. Humidity confluence was observed during all fog events and results in mist formation. Finally, a change in wind direction and formation of an air current from the river region contributes additional humidity for fog formation. Only one event was calm. This calm condition was an additional mechanism of the humidity accumulation at low levels. In this event and two others precipitation occurred before the fog, contributing to humidification of the air by evaporation from the humid surface and raindrops. This is an additional mechanism of fog formation. A warmer sea surface contributes to more evaporation and, as a consequence, increases the amount of water vapor in the surrounding air at low levels near the coast. Positive latent heat flux results in a humidity increase and, therefore, moisture accumulation in the coastal region. Negative sensible heat flux results in air cooling, possible water vapor condensation, and, finally, fog formation.

The absence of the intertropical convergence zone, frontal zones, and upper tropospheric cyclonic vortex in the study region was confirmed by the air current at the principal levels, satellite imagery, and temperature and moisture advection. All this shows the possibility of using the PAFOG model for fog events.

The PAFOG model was used whenever possible. It was not used for five events, because of the absence of initial WRF data for one and rain before four others. Therefore, the PAFOG model was used for three events. The forecast was satisfactory for two cases and not for one. Satisfactory results for fog duration and intensity were obtained with 9 h antecedence.

There was no significant effect of vegetation conditions (fast-growing sugarcane) on the low visibility forecast by the PAFOG model. However, a trend of more precise forecasting of visibility, fog duration, and event initiation with use of maximum

Table 4

Visibility (V), fog duration (D), and antecedence (A) forecast by the PAFOG model, using standard vegetation conditions (S) and vegetation variables (1, 2, …, 8) for Maceio, 12 April 2002

	S	Vegetation variables															
		1st		2nd		3rd		4th		5th		6th		7th		8th	
		L	H	L	H	L	H	L	H	L	H	L	H	L	H	L	H
V	118	101	65	101	129	101	153	86	112	205	278	105	118	111	86	110	118
D	3	3	3	3	3	3	3	4	3	2	1	4	3	3	4	3	3
A	6	9	6	9	9	9	9	9	6	6	9	6	6	6	9	6	6

L and *H* refer to the low and high limit for the variable

water storage of foliage for Maceio (5th variable) was observed. In our opinion, the reason for the small effect of vegetation conditions on the fog forecast results is that the main mechanism of fog formation on the Northern Coast of Brazil is not typical radiation fog but a dynamic process in the atmosphere. Fog forecasting by use of the PAFOG model was not very satisfactory because of the use of calculated vertical profiles and lack of radiosonde data. Integration of the numerical model with specific local observational data is recommended for future study development.

Acknowledgments

REFERENCES

ALMEIDA, A.C.S., SOUZA, J.L.; TEODORO, I.; BARBOSA, G.V.S., MOURA FILHO G., FERREIRA JÚNIOR, R.A., 2008. Desenvolvimento vegetativo e produção de cana-de-açúcar em relação à disponibilidade hídrica e unidades térmicas. Ciênc. agrotec., Lavras, *32*(5), 1441–1448.

BERGOT, T., CARRER D., NOILHAN, J, BOUGEAULT, P., 2005. *Improved site-specific numerical prediction of fog and low clouds: A feasibility study*. Weather and Forecasting, *20*, 627–646.

BOTT, A., TRAUTMANN, T., 2002. *PAFOG–A new efficient forecast model of radiation fog and low level stratiform clouds*. Atmos. Res. *64*, 191–203, 2002.

BOTT, A., SIEVERS, U., ZDUNKOWSKI, W., 1990. *A radiation fog model with a detailed treatment of the interaction between radiative transfer and fog microphysics*. J. Atmos. Sci. *47*, 2153–2166.

BYERS, H.R., 1959. General Meteorology, Synoptic and aeronautical meteorology. MC Graw Hill Company: New York.

COTTON, W. R., ANTHES, R.A., 1989. Storm and cloud dynamics. Academic press, Inc, New York.

DJURIC, D., 1994. Weather Analysis. New Jersey: Printice Hall, 304p.

FEDOROVA, N., LEVIT, V., FEDOROV, D., 2008. *Fog and Stratus Formation on the Coast of Brazil*. Atmospheric Research, *87*, 2008, 268–278.

FEDOROVA, N., LEVIT, V., SILVA A.O., SANTOS D.M.B., 2013. *Low Visibility Formation and Forecasting on the Northern Coast of Brazil*. Pure and Applied Geophysics, *170*(4), 689–709.

FERREIRA JUNIOR, R.A., SOUZA, J.L., LYRA, G.B., TEODORO, I., SANTOS, M. A., PORFIRIO, A.C.S., 2012. *Crescimento e fotossíntese de cana-de-açúcar em função de variáveis biométricas e meteorológicas, Revista Brasileira de Engenharia Agrícola e Ambiental*, *16*(11), 1229–1236.

FU, G., ZHANG, S., GAO, S., LI., P., 2012. Understanding of Sea Fog over the China Seas. Ocean University of China. China.

GOMES, H.B., FEDOROVA N., LEVIT V., 2011. *Rare events of stratus clouds on the northeast coast of Brazil*. Revista Brasileira de Meteorologia, *26*(1), 9–18.

GULTEPE, I., MULLER, M.D., BOYBEYI, Z., 2006. *A new visibility parameterization for warm fog applications in numerical weather prediction models*. J. Appl. Met. Clim., *45*, 1469–1480.

GULTEPE I., TARDIF R., MICHAELIDES S. C., CERMAK J., BOTT A., BENDIX J., MULLER M.D., PAGOWSKI M., HANSEN B., ELLROD G., JACOBS W., TOTH G., COBER S. G. 2007. *Fog Research: A review of past achievements and future perspectives*. Pure and Applied Geophysics. *164*, 1121–1159.

GULTEPE I., PEARSON G., MILBRANDT J.A., HANSEN B., PLATNICK S., TAYLOR P., GORDON M., OAKLEY J.P., COBER S. G. 2009. The fog remote sensing and modeling field project. AMS, BAMS, 342–359.

GUSEVA, N.N., RAZIMOR, M.Y., 1986. Fog and visibility forecasting. Short-term Weather Forecasting. Hydrometeoisdat, Leningrad (in Russian).

KOUSKY, V. E., 1979. *Frontal influences on northeast Brazil*. Mon. Wea. Rev., *107*(9), 1140–1153.

KOUSKY, V. E., GAN, M. A., 1981. *Upper tropospheric cyclonic vortices in the tropical South Atlantic*. Tellus, *33*(6), 538–551.

KUNKEL, B. A., 1984. *Parametrization of droplet terminal velocity and extinction coefficient in fog models*. J. Clim. Appl. Met., *23*, 34–41.

MELLOR, G.L., YAMADA, T., 1982. *Development of a turbulence closure model for geophysical fluid problems*. Rev. Geophys. Space Phys. *20*, 851–875.

MOLION, L.C.B.; BERNARDO, S.O., 2002 *Uma revisão da dinâmica das chuvas no Nordeste Brasileiro*. Revista Brasileira de Meteorologia, *17*(1),1–10.

PETTERSSEN, S., 1956. Motion and motion systems. weather and weather systems. In: Weather Analysis and Forecasting, vol.*1*, vol. *2*. McGraw-Hill, New York, Toronto, London. 266p.

PIVA, E.D., FEDOROVA, N., 1999. *Um Estudo sobre a formação de nevoeiro de radiação em Porto Alegre*. Revista Brasileira de Meteorologia *14*(2), 47–62.

RATISBONA, L.R., 1976. The climate of Brazil. Chapter 5. In: Schwerdtfeger, W. (Ed.), Climates of Central and South America. Elsevier Scientific Publishing Company, Oxford, pp. 219–269.

ROBERTSON, M.J., INMAN-BAMBER, N.G., MUCHOW, R.C., WOOD A.W., 1999. *Physiology and productivity of sugarcane with early and mid-season water deficit*. Field Crops Research, *64*, 211–227.

RODRIGUES, L. R. L., FEDOROVA, N., LEVIT, V., 2010. Adverse meteorological phenomena associated with low level baric troughs in the Alagoas State in 2003. Atmospheric Science Letters, doi:10.1002/asl.273.

SANTOS, M.A., SOUZA, J.L., LYRA G.B., TEODORO, I., FERREIRA J.R.A, PORFIRIO, A.C.S., 2008. Componentes da radiação solar em cultivo de cana-de-açúcar na região dos Tabuleiros costeiros de Alagoas. In: 9 Congresso Nacional da STAB, 2008, Maceió, CD.

SIEBERT, J., BOTT, A., ZDUNKOWSKI, W., 1992. *Influence of a vegetation-soil model on the simulation of radiation fog*. Beitr. Phys. Atmos. *65*, 93–106.

SILVEIRA, P.S., 2003. Analysis of the fog cases and Stratus clouds in Airport of Maceio. M.Sc. Thesis, Federal University of Alagoas, Maceio, Brazil.

VASQUEZ, T. 2000, Weather Forecasting Handbook. Garland, Texas: Weather Graphics Technologies, 98p.

WELCH, R.M., RAVICHANDRAN, 1986. *Prediction of quasi-periodic oscillations in radiation fogs, Part I: Comparison of simple similarity approaches*. J. Atmos. Sci., *43*, 633–651.

WILLETT, 1928. *Fog and haze, their causes, distribution and forecasting*. Mon. Wea. Rev., *56*, 435–468.

ZDUNKOWSKI, W.G., PANHANS, W.-G., WELCH, R.M., KORB, G.J., 1982. *A radiation scheme for circulation and climate models*. Beitr. Phys. Atmos. *55*, 215–238.

ZHOU, B. and B. S. FERRIER, 2008. *Asymptotic analysis of equilibrium in radiation fog*. J. Appl. Meteor. Clim., *47*, 1704–1722.

ZHOU, B. and DU J., 2010. *Fog prediction from a multimodel mesoscale ensemble prediction system*. Weather and Forecasting, *25*, 303–322.

ZHOU, B., DU, J., DIMEGO, G., 2011. *Forecast of low visibility and fog from NCEP: current status and efforts*, Pure Appl. Geophys, doi:10.1007/s00024-011-0327-x.